ADVANCING EARTH AND SPACE SCIENCES

Geophysical Research Letters

RESEARCH LETTER
10.1029/2025GL119496

Integrating Diurnal Pulsing Signatures for AI-Driven Tropical Cyclone Intensity Prediction

Xinyan Zhang[1], Jing-Yi Zhuo[2], Xuwei Bao[1], Zhe-Min Tan[3], Shan Guo[4], and Kexin Zhu[5]

[1]Shanghai Typhoon Institute, China Meteorological Administration, Shanghai, China, [2]High Meadows Environmental Institute, Princeton University, Princeton, NJ, USA, [3]School of Atmospheric Sciences, Nanjing University, Nanjing, China, [4]Shanghai Academy of Artificial Intelligence for Science, Shanghai, China, [5]School of Atmospheric Sciences, Sun Yat-sen University, Zhuhai, China

Key Points:

- Integration of diurnal pulse features into AI models substantially enhances TC intensity prediction, particularly for rapid intensification
- Diurnal pluses exhibit superior predictive skill compared to conventional instantaneous convective indicators in TC intensity forecasts
- Persistent diurnal pulse activity serves as a robust precursor for subsequent rapid intensification forecasting in TCs

Supporting Information:

Supporting Information may be found in the online version of this article.

Correspondence to:

X. Bao and Z.-M. Tan,
baoxw@typhoon.org.cn;
zmtan@nju.edu.cn

Citation:

Zhang, X., Zhuo, J.-Y., Bao, X., Tan, Z.-M., Guo, S., & Zhu, K. (2026). Integrating diurnal pulsing signatures for AI-driven tropical cyclone intensity prediction. *Geophysical Research Letters*, *53*, e2025GL119496. https://doi.org/10.1029/2025GL119496

Received 18 SEP 2025
Accepted 12 FEB 2026

Author Contributions:

Conceptualization: Xuwei Bao
Data curation: Xinyan Zhang
Formal analysis: Xinyan Zhang
Funding acquisition: Xinyan Zhang, Xuwei Bao
Investigation: Xinyan Zhang
Methodology: Xinyan Zhang, Kexin Zhu
Project administration: Xuwei Bao
Software: Shan Guo
Supervision: Xuwei Bao, Zhe-Min Tan
Validation: Shan Guo
Writing – original draft: Xinyan Zhang
Writing – review & editing: Jing-Yi Zhuo, Xuwei Bao, Zhe-Min Tan

Abstract Although artificial intelligence (AI) models are increasingly applied to tropical cyclone (TC) intensity prediction, they predominantly rely on instantaneous meteorological variables (e.g., satellite infrared images) while often overlooking more informative temporal evolution signals, such as convective diurnal variation. The diurnal pulse (DP), a daily-scale expansion of TC upper-level cold clouds, effectively captures the spatiotemporal evolution of TC convection and is tightly linked to TC intensity changes, particularly rapid intensification (RI). By incorporating the DP as a temporal evolution signal, AI models achieved significantly improved prediction skill for TC intensification rates and RI probabilities, outperforming those using only conventional instantaneous convective indicators. Permutation tests further confirm that the DP predictors contribute more pronouncedly to forecast skill than instantaneous convective proxies. These findings highlight the untapped potential of incorporating physics-informed, continuous temporal evolution variables into AI models to improve TC intensity forecasting, especially for challenging RI events.

Plain Language Summary Predicting the intensity change of tropical cyclones is challenging, as they can undergo sudden intensification or weakening within a short time. Artificial intelligence (AI) has recently emerged as a promising tool for improving tropical cyclone (TC) intensity forecasting. However, most existing AI-based models often use "snapshots" of the atmosphere, such as satellite images at single or several moments, to predict TC intensity. Such snapshots often fail to capture the continuous temporal evolution of TCs. By contrast, the diurnal pulsing process describes a sustained outward expansion of upper-level cold clouds and often occurs before TC rapid intensification. This study demonstrates that incorporating diurnal pulse features enables AI-based models to generate more accurate and reliable TC intensity forecasts, especially for rapid intensification events. These findings highlight the importance of incorporating dynamic, physics-informed signals into AI-based models to improve the TC intensity forecasting.

1. Introduction

Timely and accurate forecasting of tropical cyclone (TC) intensity changes remains a major challenge, particularly for rapid intensification (RI) events (Cangialosi et al., 2020; DeMaria et al., 2014; Leroux et al., 2018), owing to the complex multi-scale interactions between external environmental forcing and internal TC dynamics (Rogers, 2021). While favorable environmental conditions (e.g., high ocean heat content) provide the necessary thermodynamic demands for TC intensification (Hendricks et al., 2010; Kaplan & DeMaria, 2003), internal convective processes play a crucial role in RI by modulating latent-heating release and angular momentum (Fischer et al., 2020; Nguyen et al., 2017; Rogers et al., 2015, 2016). Numerous studies have identified various convective indicators for RI prediction, including deep convective bursts (Guimond et al., 2010; Vigh & Schubert, 2009), convection distribution patterns (Alvey Iii et al., 2015; Stevenson et al., 2018; Susca-Lopata et al., 2015; Xu et al., 2017), and cloud and precipitation symmetry coverage (Kieper & Jiang, 2012; Ruan & Wu, 2018; Tao & Jiang, 2015). However, these indicators primarily capture instantaneous states of convective structures rather than the temporally evolving convective processes underlying TC intensity changes, which are unable to express the cumulative effect of these processes. Notably, intense convective signals may occur at both the onset and near the end of TC intensification, reducing their specificity as a reliable predictor of RI (Shi et al., 2023; Tao & Jiang, 2015). In contrast, recent studies suggest that diurnal variations in TC convection, largely driven by radiative effects, offer more valuable temporal evolution signals for RI prediction (Sun et al., 2021; Wu et al., 2020, 2025; Zhang & Xu, 2021, 2023, 2024).

The diurnal pulse (hereafter DP) of TC upper-level cold clouds stands out as the most prominent manifestation of TC diurnal convective variability, characterized by a radially outward propagation of cloud-top cooling signatures throughout the day (Ditchek et al., 2019; Dunion et al., 2014; Zhang et al., 2023; Zhang & Xu, 2021). Notably, Zhang and Xu (2021) reported that TCs approaching or undergoing RI often possess significantly stronger and longer-lived DP events than those in non-RI TCs. Specifically, 70%–80% of RI TCs experience long-duration (>15 hr) DP events before the RI onset, suggesting DP may serve as a potential RI precursor. These DP signals are likely driven by convective gravity waves excited by the nighttime convective invigoration (Dunion et al., 2014; Navarro & Hakim, 2016; O'Neill et al., 2017). While most TCs experience nocturnal convective enhancement, a long-lived DP typically develops only when the released heating effectively excites gravity waves that remain strongly coupled to the convection within TCs. Such long-lived DPs, particularly those that persist beyond a certain temporal threshold (e.g., >15 hr), may subsequently enhance the secondary circulation and vertical coupling within the vortex, fostering convective deepening and vortex symmetrization while reducing vortex tilt (Alvey Iii & Hazelton, 2022; Zhang & Xu, 2024). This accumulated positive feedback facilitates further intensification of TCs. These findings collectively indicate that TC intensity changes are significantly influenced by processes such as the DP, rather than merely depending on the instantaneous intensity or distribution of TC convection. Despite these robust correlations between DPs and TC intensification, it remains uncertain whether and how to effectively incorporate DP information to improve TC intensity forecasting.

Statistical–dynamical models have been widely adopted in operational TC intensity forecasting due to their computational efficiency and reasonable performance. The Statistical Hurricane Intensity Prediction Scheme (SHIPS) represents one of the most established examples, utilizing a rather comprehensive set of environmental, structural, and climatological predictors to provide deterministic intensity forecasts and RI probability predictions (DeMaria et al., 2005; DeMaria & Kaplan, 1994; Kaplan et al., 2015). The SHIPS framework incorporates numerous convective indicators associated with TC intensity change, including principal component and standard deviation of infrared brightness temperature fields, azimuthally average brightness temperatures, precipitable water, and so on (Kaplan et al., 2015). However, the majority of these predictors used in SHIPS primarily represent an instantaneous state of oceanic or atmospheric conditions that fail to capture the temporally evolving processes like DP.

In recent years, artificial intelligence (AI) techniques have gained prominence in TC intensity forecasting because of their ability to process heterogeneous data and capture inherently complex nonlinear relationships (Li et al., 2024; Lian et al., 2025; Meng et al., 2023; Wang et al., 2024; Xu et al., 2021). While advancements in computational efficiency and algorithms have dramatically enhanced AI-model performance, the careful selection and integration of physically meaningful prior knowledge remain critical. For example, recent studies have successfully introduced TC internal structural features tightly related to intensity changes into AI models, such as storm asymmetry (Hu et al., 2020; Tian et al., 2025), deep convective cloud coverage (Wu et al., 2025), surplus precipitation relative to neutral TCs (Su et al., 2020), and the TC fullness (Zhuo & Tan, 2021). Notably, Wu et al. (2025) demonstrated that including hourly deep convective cloud coverage in AI models improves TC RI forecasts, highlighting the importance of resolving diurnal-scale structural evolution. Despite these advances, current AI models typically rely on inputs that reflect the static states (instantaneous intensity and structure), underutilizing dynamic evolution signals such as DPs. As one of the most prominent diurnal features and a proven precursor to subsequent TC intensification (Zhang & Xu, 2021), the DP remains an untapped opportunity to further enhance the predictive accuracy of AI-based models.

This study investigates whether incorporating the DP signature into an AI model can improve TC intensity change forecasts. Among various AI-based models, long short-term memory (LSTM) networks are particularly effective for capturing sequential dependencies and have demonstrated success in TC-related applications (Chen et al., 2023; Yang et al., 2020; Zhou et al., 2024). Therefore, this study proposes a light AI-based model using an LSTM network combined with an attention mechanism, and adds the physics-based DP into the input representation. The model performance is then evaluated using various metrics, and the specific contribution of DP features is quantitatively assessed.

10.1029/2025GL119496

2. Data and Method

2.1. Data

TC best track data were extracted from the National Hurricane Center and the U.S. Navy's Joint Typhoon Warning Center in the version-4 International Best Track Archive for Climate Stewardship (IBTrACs, Knapp et al., 2010, 2018). Cloud-top infrared brightness temperatures (IR BTs) were retrieved from the Gridded Satellite B1 (GridSat) data set of the National Oceanic and Atmospheric Administration (NOAA) Climate Data Record program (Knapp et al., 2011). This study uses the IR BT data in the 11-μm channel with a spatial resolution of 0.07° and a temporal resolution of 3 hr. The environmental variables are derived from the fifth generation of European Center for Medium-Range Weather Forecasts reanalysis data (ERA5; Hersbach et al., 2020), which provides hourly estimates of meteorological variables at a spatial resolution of 0.25°.

2.2. Design of the Model Input

This study compiles a global data set from 2001 to 2018 that includes TC best track, environmental conditions, instantaneous convective proxies, and DP features. Note that this data set includes all TCs whose complete life cycles occurred within 2001–2018, thereby excluding storms that spanned across the calendar years (e.g., forming in late 2018 and dissipating in early 2019). A set of predictors from multi-source data sets was calculated as model input for forecasting TC intensity change. TC state records are obtained from the best track data set and include the current intensity (1-min average maximum sustained wind), the previous 12-hr intensity change, center position (latitude and longitude), and its distance to land. While latitude and longitude are not physical drivers of TC intensity change, they are included to help the model distinguish between different background regimes across ocean basins. Meanwhile, environmental predictors are derived from the ERA5 reanalysis and include sea surface temperatures (SST), 200–850 hPa vertical wind shear, 200-hPa divergence, and 850-hPa vorticity. Convective structural features are derived from Gridsat-B1, including the inner-core (0–100 km) mean IR BTs and the fractional coverage of deep convective clouds, defined as the area with IR BT below 208 K within 200 km of the storm center. These features reflect the intensity and distribution of TC convection (Wu et al., 2025; Zhang & Xu, 2021). To capture the diurnal variation of TC convection, two DP features are incorporated into the model: DP duration and DP amplitude. The DP duration quantifies the total accumulated time of cold cloud propagation observed within the previous 24 hr up to the analysis time, while the DP amplitude quantifies the magnitude of cloud-top cooling associated with the DP. Both features reflect the strength of the DP and are extracted using the objective identification method proposed by Zhang et al. (2023). Although previous studies typically define a DP event as one lasting longer than 6–9 hr (Ditchek et al., 2019; Zhang et al., 2023), this study incorporates both duration and amplitude without imposing a strict threshold for what constitutes a DP event. As a result, all TCs are represented consistently, regardless of whether they exhibit distinct DP events. The detailed methodology for identifying these DP characteristics is described in (Figure S1 of Supporting Information S1).

The predictors used in this study can be grouped into four categories: TC states (intensity, previous 12-hr intensity change, latitude, longitude, and distance to land), environmental factors (SST, vertical wind shear, 200-hPa divergence, and 850-hPa vorticity), instantaneous convective proxies (inner-core IR BT, deep cloud coverage), and DP features (DP duration, DP amplitude) (Figure 1). DP features capture the daily evolution of convection, whereas convective proxies describe its instantaneous state. All predictors are computed every 3 hr. To enable the model to resolve diurnal variation processes, each training sample is a daily-length sequence of eight consecutive 3-hourly records ($x_{t0}, x_{t0-3}, \cdots x_{t0-21}$), as used to predict the TC intensity change in the next 6, 12, 18, and 24 hr ($Y_{t0+6}, Y_{t0+12}, Y_{t0+18}, Y_{t0+24}$). Only TCs that remained over water (minimum distance to land >0) and were classified as tropical or subtropical storms throughout the forecast interval are included in our data set. The sample sizes are listed in Table 1, and detailed definitions of all predictors are provided in Table S1 of Supporting Information S1.

2.3. Deep Learning Model Architecture

A lightweight, multi-task deep learning model that couples LSTM layers with an attention mechanism was developed to ingest multivariate time-series data (Figure 1). The LSTM network is specifically designed to capture time dependencies in sequential data (Hochreiter & Schmidhuber, 1997). It introduces memory cells and gating mechanisms to selectively retain or discard information over time, making it effective for learning patterns in time series data. In addition, attention mechanisms allow the model to dynamically focus on specific parts of

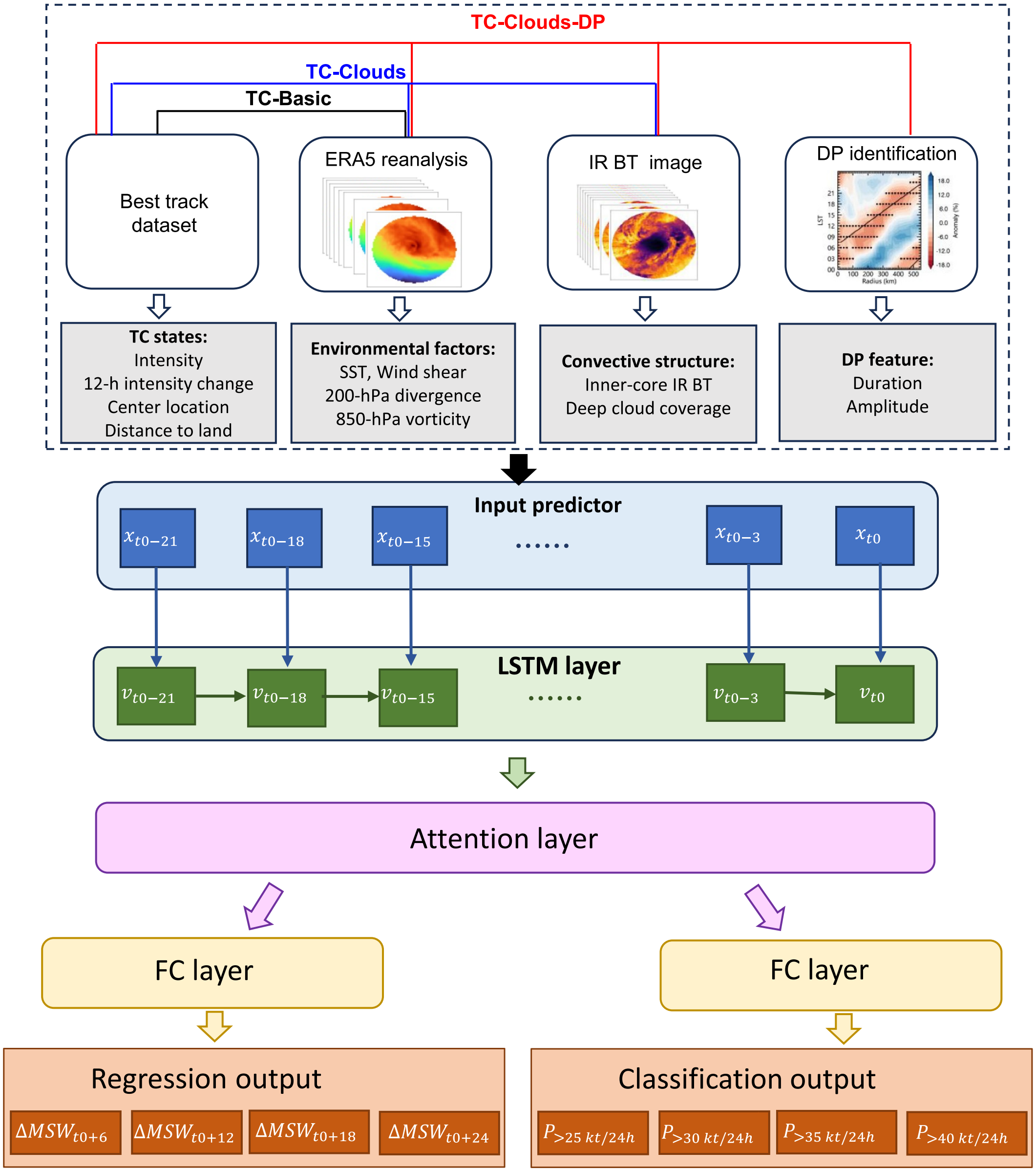

Figure 1. Schematic diagram of the model architecture. The input predictors of TC-Basic, TC-Clouds, and TC-Clouds-DP experiments are marked in the dashed box.

the input sequence (Vaswani et al., 2017), enabling the model to access relevant information from any time step directly. Integrating attention mechanisms with LSTM networks aims to enhance the model's ability to process complex sequential data.

In this framework, daily-length sequences of predictors calculated from multi-modal data (Section 2.2) are encoded by the LSTM layer and then refined by the attention layer to emphasize prominent temporal patterns. Finally, the output of the attention layer is fed into two parallel, fully-connected output branches:

1. Regression branch predicts TC intensity changes at lead times of 6, 12, 18, and 24 hr.
2. Classification branch estimates the probabilities of RI events, defined by intensification exceeding thresholds of 25, 30, 35, and 40 kt in the future 24 hr.

This multi-task learning framework enables the model to concurrently capture both fine-grained intensity change distributions and RI probabilities, thereby improving generalization performance for both prediction tasks.

Table 1
Mean Absolute Error (MAE; kt) of Intensity Change Forecasts Across all Basins for the TC-Basic, TC-Clouds, and TC-Clouds-DP Experiments, Based on Cross Tests From 2001 to 2018

Basin	Sample size	Model interval	TC-basic	TC-clouds	TC-clouds-DP
NWP	10,422	6 h	3.75	3.71	**3.60**$^{*+}$
		12 h	6.61	6.53^{+}	**6.30**$^{*+}$
		18 h	9.04	8.92^{+}	**8.60**$^{*+}$
		24 h	11.20	11.06^{+}	**10.61**$^{*+}$
NEP	8,231	6 h	2.84	2.81	**2.75**
		12 h	4.96	4.93	**4.76**$^{*+}$
		18 h	6.66	6.60^{+}	**6.35**$^{*+}$
		24 h	8.08	7.97^{+}	**7.66**$^{*+}$
NA	6,115	6 h	3.21	3.16^{+}	**3.04**$^{+}$
		12 h	5.83	5.73^{+}	**5.39**$^{*+}$
		18 h	8.07	7.96^{+}	**7.36**$^{*+}$
		24 h	10.01	9.86^{+}	**9.15**$^{*+}$
SH	9,205	6 h	3.46	3.44	**3.33**$^{*+}$
		12 h	6.15	6.12	**5.88**$^{*+}$
		18 h	8.48	8.40^{+}	**8.07**$^{*+}$
		24 h	10.51	10.35^{+}	**10.06**$^{*+}$

Note. The lowest MAE is highlighted in bold. "*" indicates that the MAE is significantly lower than that of the TC-Clouds at the 95% confidence level based on a Student-t test, while "$^{+}$" denotes a significant improvement over the TC-Basic.

Comparative analyses of multi-task, regression, and classification approaches (Figure S2 and Table S3 in Supporting Information S1) demonstrate that multi-task learning effectively mitigates the smoothing effect of regression loss on infrequent RI events, while simultaneously enhancing the reliability of RI probability classification. A weighted loss function is employed to mitigate the class imbalance between RI and non-RI cases and reconcile regression and classification losses. Complete specifications of the optimization algorithm, loss function formulation, and hyperparameter configurations are provided in Supporting Information S1.

2.4. Experimental Setup and Evaluation Metrics

To quantify the added skill of TC intensity forecast contributed by DP features, three sets of experiments are conducted to compare the model's performance with different input predictors: TC-Basic, TC-Clouds, and TC-Clouds-DP. As shown in Figure 1, the TC-Basic model only inputs 3-hourly series of TC state records and environmental factors. The TC-Clouds model extends the TC-Basic model by adding convective structure metrics (inner-core IR BT and deep cloud coverage). The TC-Clouds-DP further supplements TC-Clouds with the DP duration and amplitude features. Following previous studies (Eusebi et al., 2025; Vabalas et al., 2019), model performance is evaluated using a nested leave-1-yr-out validation and testing framework applied to the period from 2001 to 2018. This approach ensures comprehensive evaluation across the full data set. The detailed procedure of this cross-validation and test process is provided in Supporting Information S1.

Since TC activity and RI climatology vary greatly across ocean basins, the evaluation is performed separately for the four major TC basins: Northwest Pacific (NWP), Northeast Pacific (NEP), North Atlantic (NA), and South Hemisphere (SH). The corresponding sample size for each basin is shown in Table 1. The mean absolute error (MAE) is calculated to quantify the forecast error for the TC intensity change rate. For probabilistic RI forecast, the forecasting skill is evaluated using Brier skill score (BSS) and F1 score. In addition, to explore how much the introduced DPs contribute to the model performance, the permutation test is performed to quantify the importance of each input predictor. The detailed description of these evaluation metrics is provided in Supporting Information S1. To evaluate model performances against an existing benchmark, the model predictions are matched and compared to the real-time operational forecast from SHIPS, and the results are provided in Table S4 and Figure S4 of Supporting Information S1.

3. Results

3.1. Evaluation of Model Performance

Table 1 shows the MAE of 6,12, 18, and 24-hr intensity forecasts for TCs based on the leave-1-yr-out test across the data set from 2001 to 2018 from the TC-Basic, TC-Clouds, and TC-Clouds-DP experiments. Among the four basins, the forecast error in the NWP is the largest, possibly due to the highest frequency of RI events among TCs in this basin. The TC-Basic model, which uses only TC states and environmental factors, has the largest MAE across all basins and lead times. Adding convective-structure predictors (TC-Clouds) reduces the MAE by about 1%–3% at all lead times relative to TC-Basic. Further inclusion of the DP features leads to the best performance overall. The TC-Clouds-DP model achieves the lowest MAE across all lead times in nearly every basin, demonstrating a significant improvement of 4%–7% relative to TC-Basic and 2%–5% relative to TC-Clouds. The performance gain is especially notable at longer lead times (18–24 hr), indicating the added value of DP information in capturing the long-term intensity evolution of TCs.

Figures 2a–2c compare the 24-hr intensity-change forecasts of the three experiments with observations. In general, the dominant bias of all three experiments is mainly attributed to the underestimation of both RI (e.g., $\geq$25 kt/24 hr) and rapid weakening (RW) (e.g., ≤ -25 kt/24 hr). Nevertheless, the TC-Clouds-DP forecast

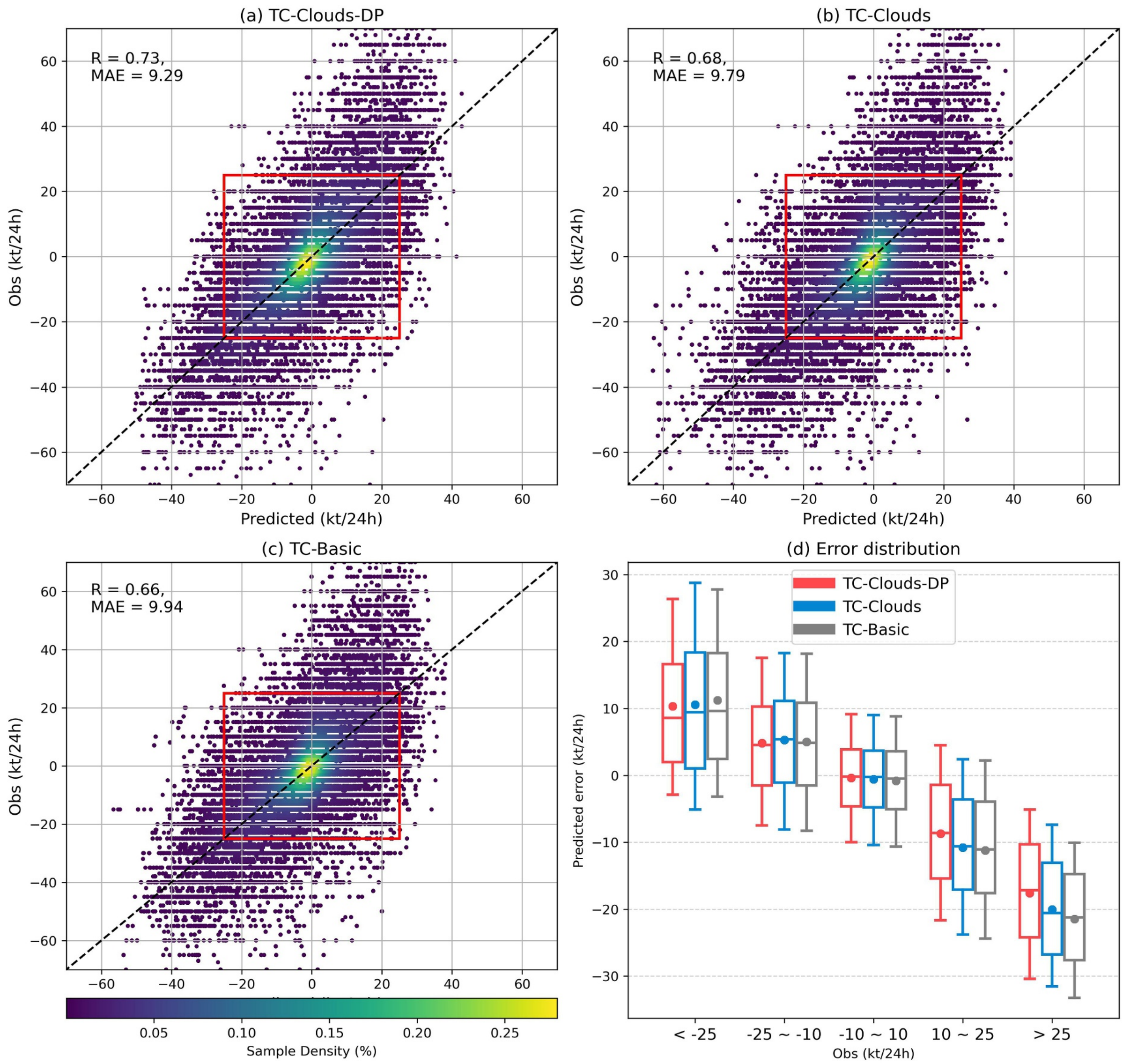

Figure 2. Scatter plot of predicted versus observed 24-hr TC intensity change based on a leave-1-yr-out test across 2001–2018 global TCs from the (a) TC-Clouds-DP, (b) TC-Clouds, and (c) TC-Basic; (d) Boxplots of model error in 24-hr intensity change for three experiments. Whiskers, boxes, median lines, and dots in the boxplot represent the upper and lower bounds (90%, 10%), interquartile range (75%, 25%), median (50%), and mean value of the TC intensity. The correlation coefficient (R) and mean absolute error of each experiment are marked at the upper left in (a–c); Red boxes highlight the region where both observation and predicted intensity change within ±25 kt/24 hr.

samples show markedly better alignment with the 1:1 line, especially in the RI and RW distribution tails. The boxplots stratified by observed 24-hr intensity-change bins further illustrate the systematic improvement achieved by TC-Clouds-DP (Figure 2d). Across all bins from rapid weakening (<−25 kt/24hr) to rapid intensification (>25 kt/24 hr), TC-Clouds-DP yields smaller median errors and narrower interquartile ranges relative to the other two models, especially for intensifying storms (>10 kt and >25 kt). As a result, the TC-Clouds-DP attains the highest forecast-observation correlation ($r = 0.73$; Figure 2a), followed by the TC-Clouds ($r = 0.69$; Figure 2b) and TC-Basic ($r = 0.68$; Figure 2c). These results suggest that introducing DP features into the model could improve the ability to capture rapid TC intensity changes (both RI and RW), leading to more accurate intensity forecasts.

Given its superior capability to capture rapid TC intensity changes, TC-Clouds-DP exhibits the highest skill in RI probability forecasting. Figure 3 shows the tested BSS and F1 score across different RI thresholds for the three experiments in NWP (Figures 3a and 3b), NEP (Figures 3c and 3d), NA (Figures 3e and 3f), and SH (Figures 3g

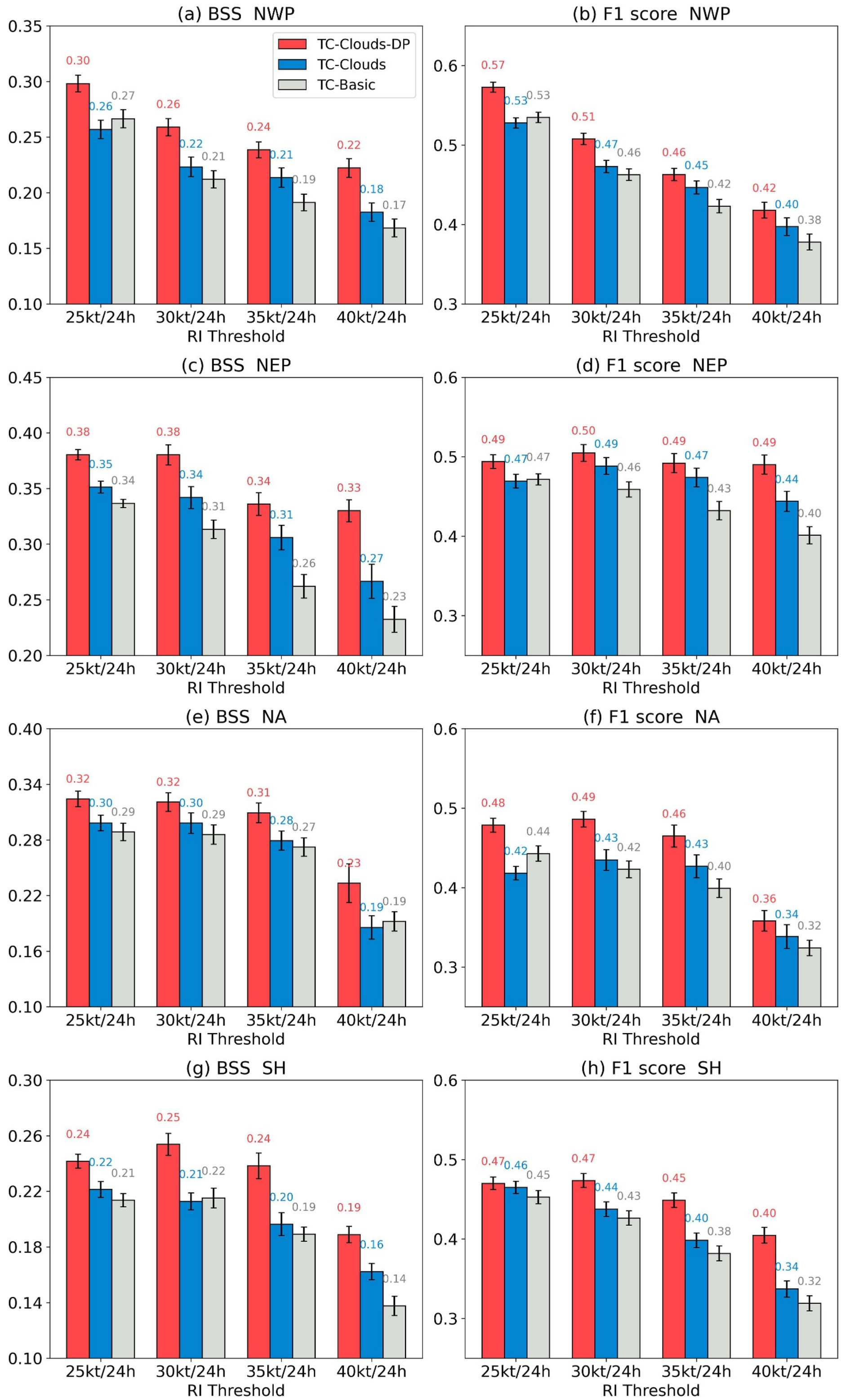

Figure 3. Brier skill score and F1 score of RI probability forecasts from the TC-Clouds-DP (red bars), TC-Clouds (blue bars), and TC-Basic (white bars) experiments in (a, b) NWP, (c, d) NEP, (e, f) NA, and (g–h) SH. Uncertainty bars indicate 95% confidence intervals from the 18-yr cross-validation results.

and 3h) basins. Across all RI thresholds and basins, TC-Clouds-DP consistently outperforms the other models, achieving BSS values of 0.2–0.35 and F1 scores of 0.4–0.5, while TC-Basic generally performs worst. Although predicting RI becomes more challenging at higher thresholds (35–40 kt/24 hr), where all models show relatively low skill scores, TC-Clouds-DP still exhibits the most substantial improvement, with skill gains of 5%–20% over TC-Clouds and 10%–30% over TC-Basic. The reliability diagram (Figure S3 in Supporting Information S1) indicates that the TC-Clouds-DP model remains well-calibrated with the observed RI frequency, while TC-Clouds shows a tendency toward increasing false alarms in the high-probability range.

3.2. Contributions of DP

Although TC-Clouds-DP demonstrates superior performance in both TC intensity change and RI prediction tasks, the specific contribution of the DP requires further quantification. Figures 4a and 4b show the 10 most influential predictors for these tasks based on the permutation test (Section 2.4). Current intensity (maximum sustained wind; referred to as MSW in Figures 4a and 4b) and SST emerge as the top two predictors for both intensity change and RI prediction. Predictors related to TC states, including the distance to the land, previous 12-hr intensity change (12-hr ΔMSW in Figures 4a and 4b), and center locations (longitude and latitude), also contribute substantially to the model performance. Note that the relatively high importance of latitude and longitude likely reflects their role in identifying basin-dependent climatological TC activity and thermodynamic conditions. While this improves model performance, geographic coordinates are not physical drivers of intensity change and should be interpreted with caution. Among the remaining predictors, DP features (DP duration and DP amplitude) make the largest additional contribution to the forecast accuracy, outperforming that of instantaneous convective structure indicators (inner-core IR BT and deep cloud coverage), vertical wind shears, and other environmental conditions (200-hPa divergence and 850-hPa vorticity). For RI prediction specifically, the DP duration ranks just after SST and TC state variables, while the DP amplitude plays a relatively limited role.

Note that the TC-Clouds-DP outperforms TC-Clouds, even though the latter already incorporates instantaneous convective structure features (inner-core IR BT and deep cloud coverage). This raises a critical question: what unique predictive values do these DP features provide beyond the instantaneous convective features? To address this, Figures 4c and 4d examine the relationship between two convective variables and two DP features with subsequent 24-hr TC intensity changes. The result reveals that the inner-core IR BT and deep cloud coverage correlate highly with both TC intensification and weakening (Figure 4c), as both RI and RW TCs similarly exhibit low IR BT and large deep cloud coverage, which may explain the false alarm of higher RI probabilities as shown in the reliability diagram (Figure S3 in Supporting Information S1). This means that these metrics primarily reflect convective activity rather than predictive information about the direction of intensity change. In contrast, the DP duration increases significantly with the intensification rate, peaking at the RI stage, while its amplitude decreases (Figure 4d). RI TCs typically exhibit DP events with an average duration exceeding 15 hr and amplitudes below -1 K, whereas weakening TCs show significantly shorter and weaker DP signatures, with little variation across weakening rates. This demonstrates a physical linkage between DP features and distinct TC intensity changes (RI and RW), which in turn contributes to more reliable TC intensity prediction (Figures 4d and 4e). These findings support the argument by Zhang and Xu (2021) that strong DP signatures can serve as TC RI precursors, whereas intense instantaneous convection is more indicative of mature TC states during the later RI stage. Figures S5 and S6 in Supporting Information S1 present two cases demonstrating this evolutionary pattern, showing pronounced DP signatures emerging prior to and during RI, followed by more organized deep convection as the TC reaches its mature phase.

Since TCs tend to produce long-duration (>15 hr) DP events (Figure 4d) prior to the RI, and since DP duration is a major contribution to RI classification (Figure 4b), the model performance is further tested exclusively on those TC samples with DP duration >15 hr (Figures 4e and 4f). Most of these TCs exhibit an intensification and even RI tendency within the subsequent 24-hr period (Figures 4e and 4f). For these TCs, the TC-Clouds shows substantial bias and systematic underestimation of intensification rate, if lacking DP information (Figure 4e). In contrast, TC-Clouds-DP reproduces the 24-hr intensity change that aligns more closely with observation, yielding both a significantly lower MAE (11.64 vs. 12.68 kt) and a higher correlation coefficient (0.74 vs. 0.67) than TC-Clouds (Figures 4e and 4f). The difference field between TC-Clouds and TC-Clouds-DP confirms that the incorporation of DP features significantly alleviates the underestimation problem and increases the probability of detecting both intensification and RI (Figure 4g). Finally, the TC-Clouds-DP achieves a more marked improvement in RI probability prediction skill than TC-Clouds for these TCs with persistent DP events (Figure 4h).

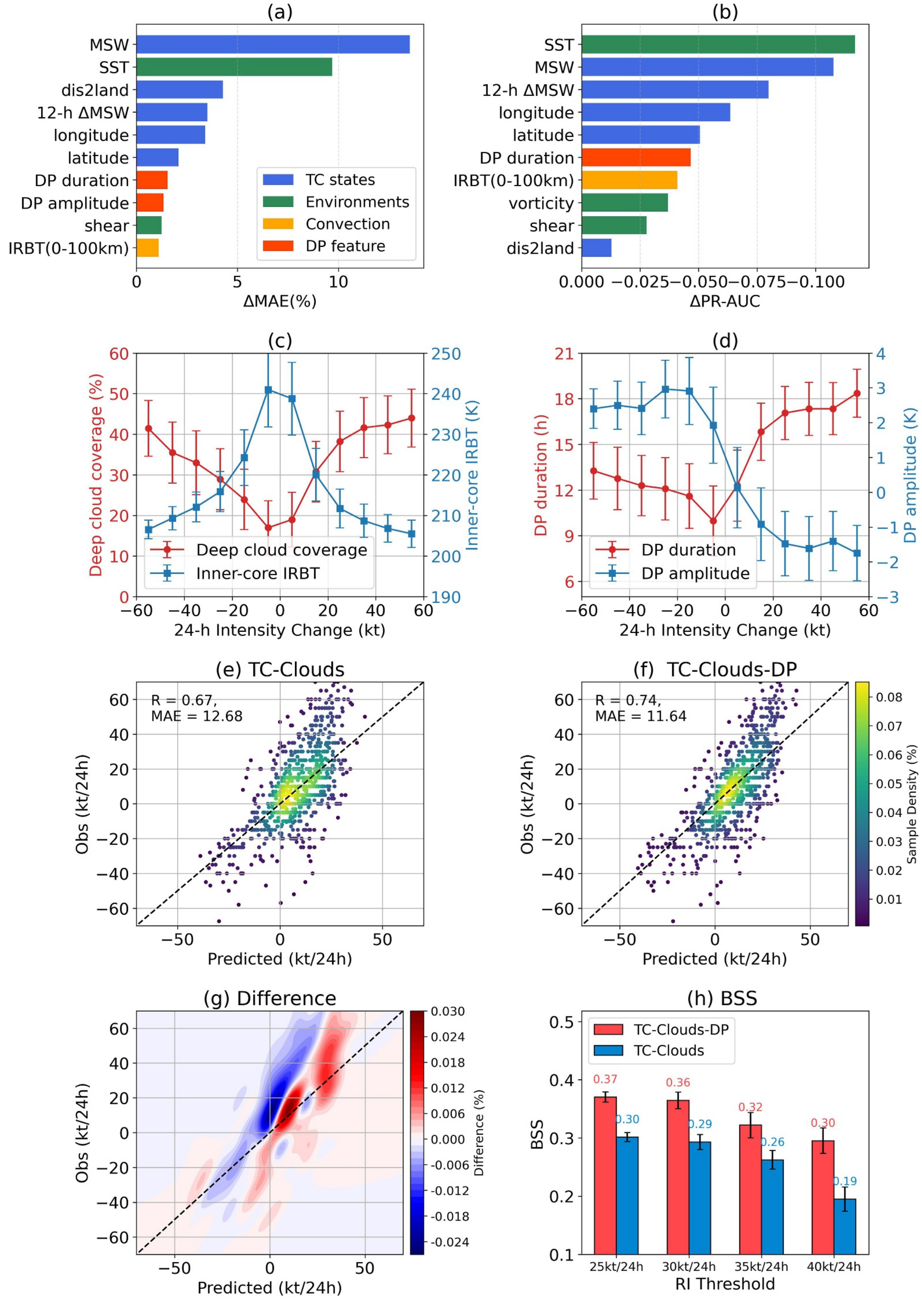

Figure 4. Ranking of the top 10 predictors by importance for (a) TC intensity change and (b) RI probability forecasting. (c, d) Convective structure metrics and DP features as a function of subsequent 24-hr TC intensity change. Scatterplots of predicted versus observed 24-hr intensity change for TC samples with long-duration (>15 hr) DP events from (e) TC-Clouds and (f) TC-Clouds-DP. (g) Density difference between the scatterplots in (e, f). (h) Brier skill score for RI probability forecasts from the TC-Clouds-DP and TC-Clouds experiments, for TC samples with long-duration (>15 hr) DP events.

4. Conclusions and Discussions

This study evaluates the contribution of DP signatures to AI-based TC intensity forecasting. A lightweight time-series model based on an LSTM network combined with an attention mechanism was used to predict both TC intensification rate and RI probability. Three experiments (TC-Basic, TC-Clouds, and TC-Clouds-DP) were designed by progressively incorporating predictors related to TC state, environmental conditions, convective structures, and DP features. Model performance was examined using nested leave-1-yr-out validation and tested across the data set from 2001 to 2018.

Among these three experiments, the TC-Clouds-DP, which incorporates DP duration and amplitude, achieves the lowest MAE in TC intensity-change forecasts at all lead times and the highest skill scores for RI probability predictions across different RI thresholds and basins. The inter-comparison of our model with the operational SHIPS forecast (Table S4 and Figure S4 in Supporting Information S1) indicates that our model not only outperforms SHIPS but also achieves skill comparable to or exceeding that of existing machine-learning approaches based on SHIPS predictors or general storm features (Eusebi et al., 2025; Su et al., 2020; Wu et al., 2025; Yang et al., 2020). Permutation importance tests show that, after SST and key TC state variables (current intensity, previous 12-hr intensity change, etc.), DP features are the most influential predictors for both TC intensity change and RI probability forecasts, outweighing the predictive value of instantaneous convective structural features (e.g., inner-core IR BT and deep cloud coverage). A possible explanation is that cold inner-core IR BTs and extensive deep cloud coverage are largely dependent on the instantaneous TC state (e.g., intensity), resulting in similar convective signatures prior to both RI and RW. In contrast, vigorous DP features (duration and amplitude) capture the spatiotemporal diurnal evolution of TC convection, which are strongly coupled with the TC intensification rate but diminish when the TC is going to weaken. Therefore, in TCs experiencing persistent DP events, incorporating DP features into the model significantly reduces the model bias and errors, leading to a marked improvement in RI probability prediction skill.

This study demonstrates the untapped potential of temporal evolution signals such as the DP to advance AI-based TC intensity forecasting. Unlike purely data-driven approaches that rely on instantaneous satellite images to infer structural changes, DPs provide the physics-informed, temporally evolving information closely linked to RI. Therefore, incorporating DP features into operational frameworks such as SHIPS may further improve real-time TC intensity forecasting. Future studies should utilize expanded data sets and more sophisticated modeling frameworks to fully resolve the spatiotemporal signatures of diurnal convection variability, thereby further improving TC intensity prediction.

Conflict of Interest

The authors declare no conflicts of interest relevant to this study.

Data Availability Statement

The IBTrACS data can be accessed from NOAA National Climatic Data Center (Knapp et al., 2018). The Gridded Satellite (GridSat) B1 data can be downloaded from the National Oceanic and Atmospheric Administration Climate Data Record program (Knapp & NOAA CDR Program, 2014). The ERA5 reanalysis data can be downloaded from the Climate Data Store (Hersbach et al., 2019). The SHIPS operational forecast data are available in the "stext" directory for each year at https://ftp.nhc.noaa.gov/atcf/archive/MESSAGES.

Acknowledgments

The authors thank Dr. Mark DeMaria and the anonymous reviewers for their constructive comments and suggestions that greatly improved the manuscript. Xuwei Bao is supported by the National Natural Science Foundation of China (U2342203), Xinyan Zhang is supported by National Natural Science Foundation of China (42505010) and the Science and Technology Commission of Shanghai (24YF2756900).

References

Alvey Iii, G. R., & Hazelton, A. (2022). How do weak, misaligned tropical cyclones evolve toward alignment? A multi-case study using the hurricane analysis and forecast system. *Journal of Geophysical Research: Atmospheres*, *127*(20), e2022JD037268. https://doi.org/10.1029/2022JD037268

Alvey Iii, G. R., Zawislak, J., & Zipser, E. (2015). Precipitation properties observed during tropical cyclone intensity change. *Monthly Weather Review*, *143*(11), 4476–4492. https://doi.org/10.1175/mwr-d-15-0065.1

Cangialosi, J. P., Blake, E., DeMaria, M., Penny, A., Latto, A., Rappaport, E., & Tallapragada, V. (2020). Recent progress in tropical cyclone intensity forecasting at the National Hurricane Center. *Weather and Forecasting*, *35*(5), 1913–1922. https://doi.org/10.1175/WAF-D-20-0059.1

Chen, B.-F., Kuo, Y.-T., & Huang, T.-S. (2023). A deep learning ensemble approach for predicting tropical cyclone rapid intensification. *Atmospheric Science Letters*, *24*(5), e1151. https://doi.org/10.1002/asl.1151

DeMaria, M., & Kaplan, J. (1994). A statistical hurricane intensity prediction scheme (SHIPS) for the Atlantic basin. *Weather and Forecasting*, *9*(2), 209–220. https://doi.org/10.1175/1520-0434(1994)009<0209:ASHIPS>2.0.CO;2

DeMaria, M., Mainelli, M., Shay, L. K., Knaff, J. A., & Kaplan, J. (2005). Further improvements to the statistical hurricane intensity prediction scheme (SHIPS). *Weather and Forecasting*, *20*(4), 531–543. https://doi.org/10.1175/WAF862.1

DeMaria, M., Sampson, C. R., Knaff, J. A., & Musgrave, K. D. (2014). Is tropical cyclone intensity guidance improving? *Bulletin of the American Meteorological Society*, *95*(3), 387–398. https://doi.org/10.1175/bams-d-12-00240.1

Ditchek, S. D., Molinari, J., Corbosiero, K. L., & Fovell, R. G. (2019). An objective climatology of tropical cyclone diurnal pulses in the Atlantic Basin. *Monthly Weather Review*, *147*(2), 591–605. https://doi.org/10.1175/mwr-d-18-0368.1

Dunion, J. P., Thorncroft, C. D., & Velden, C. S. (2014). The tropical cyclone diurnal cycle of mature hurricanes. *Monthly Weather Review*, *142*(10), 3900–3919. https://doi.org/10.1175/mwr-d-13-00191.1

Eusebi, R., Su, H., Wu, L., Rong, P., Balaguru, K., Leung, R., et al. (2025). Improving tropical cyclone rapid intensification forecasts with satellite measurements of sea surface salinity and calibrated machine learning. *Environmental Research Letters*, *20*(3), 034010. https://doi.org/10.1088/1748-9326/adac7f

Fischer, M. S., Rogers, R. F., & Reasor, P. D. (2020). The rapid intensification and eyewall replacement cycles of Hurricane Irma (2017). *Monthly Weather Review*, *148*(3), 981–1004. https://doi.org/10.1175/MWR-D-19-0185.1

Guimond, S. R., Heymsfield, G. M., & Turk, F. J. (2010). Multiscale observations of Hurricane Dennis (2005): The effects of hot towers on rapid intensification. *Journal of the Atmospheric Sciences*, *67*(3), 633–654. https://doi.org/10.1175/2009JAS3119.1

Hendricks, E. A., Peng, M. S., Fu, B., & Li, T. (2010). Quantifying environmental control on tropical cyclone intensity change. *Monthly Weather Review*, *138*(8), 3243–3271. https://doi.org/10.1175/2010mwr3185.1

Hersbach, H., Bell, B., Berrisford, P., et al. (2019). ERA5 monthly averaged data on pressure levels from 1959 to present [Dataset]. *Copernicus Climate Change Service (C3S) Climate Data Store (CDS)*. https://doi.org/10.24381/cds.6860a573

Hersbach, H., Bell, B., Berrisford, P., Hirahara, S., Horányi, A., Muñoz-Sabater, J., et al. (2020). The ERA5 global reanalysis. *Quarterly Journal of the Royal Meteorological Society*, *146*(730), 1999–2049. https://doi.org/10.1002/qj.3803

Hochreiter, S., & Schmidhuber, J. (1997). Long short-term memory. *Neural Computation*, *9*(8), 1735–1780. https://doi.org/10.1162/neco.1997.9.8.1735

Hu, L., Ritchie, E. A., & Tyo, J. S. (2020). Short-term tropical cyclone intensity forecasting from satellite imagery based on the deviation angle variance technique. *Weather and Forecasting*, *35*(1), 285–298. https://doi.org/10.1175/WAF-D-19-0102.1

Kaplan, J., & DeMaria, M. (2003). Large-scale characteristics of rapidly intensifying tropical cyclones in the North Atlantic Basin. *Weather and Forecasting*, *18*(6), 1093–1108. https://doi.org/10.1175/1520-0434(2003)018<1093:LCORIT>2.0.CO;2

Kaplan, J., Rozoff, C. M., DeMaria, M., Sampson, C. R., Kossin, J. P., Velden, C. S., et al. (2015). Evaluating environmental impacts on tropical cyclone rapid intensification predictability utilizing statistical models. *Weather and Forecasting*, *30*(5), 1374–1396. https://doi.org/10.1175/WAF-D-15-0032.1

Kieper, M. E., & Jiang, H. (2012). Predicting tropical cyclone rapid intensification using the 37 GHz ring pattern identified from passive microwave measurements. *Geophysical Research Letters*, *39*(13). https://doi.org/10.1029/2012GL052115

Knapp, K. R., & NOAA CDR Program. (2014). NOAA climate data record (CDR) of gridded satellite data from ISCCP B1 (GridSat-B1) infrared channel brightness temperature, version 2 [Dataset]. *NOAA National Centers for Environmental Information*. https://doi.org/10.7289/V59P2ZKR

Knapp, K. R., Ansari, S., Bain, C. L., Bourassa, M. A., Dickinson, M. J., Funk, C., et al. (2011). Globally gridded satellite observations for climate studies. *Bulletin of the American Meteorological Society*, *92*(7), 893–907. https://doi.org/10.1175/2011BAMS3039.1

Knapp, K. R., Diamond, H. J., Kossin, J. P., Kruk, M. C., & Schreck, C. J. (2018). International best track archive for climate stewardship (IBTrACS) project, version 4 [Dataset]. *NOAA National Centers for Environmental Information*. https://doi.org/10.25921/82ty-9e16

Knapp, K. R., Kruk, M. C., Levinson, D. H., Diamond, H. J., & Neumann, C. J. (2010). The international best track archive for climate stewardship (IBTrACS): Unifying tropical cyclone data. *Bulletin of the American Meteorological Society*, *91*(3), 363–376. https://doi.org/10.1175/2009BAMS2755.1

Leroux, M.-D., Wood, K., Elsberry, R., Cayanan, E. O., Hendricks, E., Kucas, M., & Yu, Z. (2018). Recent advances in research and forecasting of tropical cyclone track, intensity, and structure at landfall. *Tropical Cyclone Research and Review*, *7*. https://doi.org/10.6057/2018TCRR02.02

Li, W., Li, Y., Yang, Y., Song, D., Wei, Z., & Liu, A. A. (2024). Multimodal adversarial fusion for typhoon intensity forecasting. *IEEE Transactions on Geoscience and Remote Sensing*, *62*, 1–12. https://doi.org/10.1109/TGRS.2024.3367962

Lian, J., Shao, J., Yu, H., Chen, R., Huang, S., Chen, G., & Zhao, Q. (2025). Multimodal fusion learning for predicting tropical cyclone intensity over Western North Pacific. *Ieee Journal of Selected Topics in Applied Earth Observations and Remote Sensing*, *18*, 7048–7063. https://doi.org/10.1109/JSTARS.2025.3544865

Meng, F., Yao, Y., Wang, Z., Peng, S., Xu, D., & Song, T. (2023). Probabilistic forecasting of tropical cyclones intensity using machine learning model. *Environmental Research Letters*, *18*(4), 044042. https://doi.org/10.1088/1748-9326/acc8eb

Navarro, E. L., & Hakim, G. J. (2016). Idealized numerical modeling of the diurnal cycle of tropical cyclones. *Journal of the Atmospheric Sciences*, *73*(10), 4189–4201. https://doi.org/10.1175/jas-d-15-0349.1

Nguyen, L. T., Rogers, R. F., & Reasor, P. D. (2017). Thermodynamic and kinematic influences on precipitation symmetry in sheared tropical cyclones: Bertha and cristobal (2014). *Monthly Weather Review*, *145*(11), 4423–4446. https://doi.org/10.1175/mwr-d-17-0073.1

O'Neill, M., Perez-Betancourt, D., & Wing, A. (2017). Accessible environments for diurnal-period waves in simulated tropical cyclones. *Journal of the Atmospheric Sciences*, *74*. https://doi.org/10.1175/JAS-D-16-0294.1

Rogers, R. F. (2021). Recent advances in our understanding of tropical cyclone intensity change processes from airborne observations. *Atmosphere*, *12*(5), 650. https://doi.org/10.3390/atmos12050650

Rogers, R. F., Reasor, P. D., & Zhang, J. A. (2015). Multiscale structure and evolution of Hurricane Earl (2010) during rapid intensification. *Monthly Weather Review*, *143*(2), 536–562. https://doi.org/10.1175/MWR-D-14-00175.1

Rogers, R. F., Zhang, J. A., Zawislak, J., Jiang, H., Alvey, G. R., III, Zipser, E. J., & Stevenson, S. N. (2016). Observations of the structure and evolution of Hurricane Edouard (2014) during intensity change. Part II: Kinematic structure and the distribution of deep convection. *Monthly Weather Review*, *144*(9), 3355–3376. https://doi.org/10.1175/mwr-d-16-0017.1

Ruan, Z., & Wu, Q. (2018). Precipitation, convective clouds, and their connections with tropical cyclone intensity and intensity change. *Geophysical Research Letters*, *45*(2), 1098–1105. https://doi.org/10.1002/2017gl076611

Shi, D., Chen, G., & Xie, X. (2023). Revisiting the relationship between tropical cyclone rapid intensification and the distribution of inner-core precipitation. *Geophysical Research Letters*, *50*(17), e2023GL104810. https://doi.org/10.1029/2023GL104810

Stevenson, S. N., Corbosiero, K. L., DeMaria, M., & Vigh, J. L. (2018). A 10-year survey of tropical cyclone inner-core lightning bursts and their relationship to intensity change. *Weather and Forecasting*, *33*(1), 23–36. https://doi.org/10.1175/WAF-D-17-0096.1

Su, H., Wu, L., Jiang, J. H., Pai, R., Liu, A., Zhai, A. J., et al. (2020). Applying satellite observations of tropical cyclone internal structures to rapid intensification forecast with machine learning. *Geophysical Research Letters*, *47*(17), e2020GL089102. https://doi.org/10.1029/2020GL089102

Sun, L., Tang, X., Zhuge, X., Tan, Z., & Fang, J. (2021). Diurnal variation of overshooting tops in typhoons detected by Himawari-8 satellite. *Geophysical Research Letters*, *48*(21), e2021GL095565. https://doi.org/10.1029/2021gl095565

Susca-Lopata, G., Zawislak, J., Zipser, E. J., & Rogers, R. F. (2015). The role of observed environmental conditions and precipitation evolution in the rapid intensification of Hurricane Earl (2010). *Monthly Weather Review*, *143*(6), 2207–2223. https://doi.org/10.1175/MWR-D-14-00283.1

Tao, C., & Jiang, H. (2015). Distributions of shallow to very deep precipitation–convection in rapidly intensifying tropical cyclones. *Journal of Climate*, *28*(22), 8791–8824. https://doi.org/10.1175/jcli-d-14-00448.1

Tian, W., Song, P., Chen, Y., Zhang, Y., Wu, L., Zhao, H., et al. (2025). Short-term rolling prediction of tropical cyclone intensity based on multi-task learning with fusion of deviation-angle variance and satellite imagery. *Advances in Atmospheric Sciences*, *42*(1), 111–128. https://doi.org/10.1007/s00376-024-3301-0

Vabalas, A., Gowen, E., Poliakoff, E., & Casson, A. J. (2019). Machine learning algorithm validation with a limited sample size. *PLoS One*, *14*(11), e0224365. https://doi.org/10.1371/journal.pone.0224365

Vaswani, N. S., Parmar, N., Uszkoreit, J., Jones, L., Gomez, A. N., Kaiser, L., & Polosukhin, I. (2017). Attention is all you need. *arXiv: Computer Language*, 1–15.

Vigh, J. L., & Schubert, W. H. (2009). Rapid development of the tropical cyclone warm core. *Journal of the Atmospheric Sciences*, *66*(11), 3335–3350. https://doi.org/10.1175/JAS3092.1

Wang, C., Li, X., & Zheng, G. (2024). Tropical cyclone intensity forecasting using model knowledge guided deep learning model. *Environmental Research Letters*, *19*(2), 024006. https://doi.org/10.1088/1748-9326/ad1bde

Wu, Q., Hong, J., & Ruan, Z. (2020). Diurnal variations in tropical cyclone intensification. *Geophysical Research Letters*, *47*(23), e2020GL090397. https://doi.org/10.1029/2020GL090397

Wu, Q., Luo, T., & Hong, J. (2025). Incorporating hourly convective cloud data into tropical cyclone rapid intensification forecasting with machine learning. *Journal of Geophysical Research: Machine Learning and Computation*, *2*(1), e2025JH000595. https://doi.org/10.1029/2025JH000595

Xu, W., Balaguru, K., August, A., et al. (2021). Deep learning experiments for tropical cyclone intensity forecasts. *Weather and Forecasting*, *36*(4), 1453–1470. https://doi.org/10.1175/WAF-D-20-0104.1

Xu, W., Rutledge, S. A., & Zhang, W. (2017). Relationships between total lightning, deep convection, and tropical cyclone intensity change. *Journal of Geophysical Research: Atmospheres*, *122*(13), 7047–7063. https://doi.org/10.1002/2017jd027072

Yang, Q., Lee, C.-Y., & Tippett, M. K. (2020). A long short-term memory model for global rapid intensification prediction. *Weather and Forecasting*, *35*(4), 1203–1220. https://doi.org/10.1175/WAF-D-19-0199.1

Zhang, X., Ditchek, S. D., Corbosiero, K. L., & Xu, W. (2023). Global and regional characteristics of radially outward propagating tropical cyclone diurnal pulses. *Journal of Geophysical Research: Atmospheres*, *128*(7), e2022JD037660. https://doi.org/10.1029/2022jd037660

Zhang, X., & Xu, W. (2021). Diurnal variations in rainfall and precipitation asymmetry of tropical cyclones in the Northwest Pacific Region. *Journal of Climate*, 1–52. https://doi.org/10.1175/JCLI-D-20-0795.1

Zhang, X., & Xu, W. (2023). Diurnal variations on the initiation time and intensification rate of rapidly intensifying tropical cyclones. *Geophysical Research Letters*, *50*(14), e2023GL103551. https://doi.org/10.1029/2023GL103551

Zhang, X., & Xu, W. (2024). Changes in the deep convective structures of tropical cyclones associated with the diurnal pulse. *Journal of Geophysical Research: Atmospheres*, *129*(24), e2024JD041441. https://doi.org/10.1029/2024jd041441

Zhou, Y., Zhan, R., Wang, Y., Chen, P., Tan, Z., Xie, Z., & Nie, X. (2024). A physics-informed deep-learning intensity prediction scheme for tropical cyclones over the Western north Pacific. *Advances in Atmospheric Sciences*, *41*(7), 1391–1402. https://doi.org/10.1007/s00376-024-3282-z

Zhuo, J.-Y., & Tan, Z.-M. (2021). Physics-augmented deep learning to improve tropical cyclone intensity and size estimation from satellite imagery. *Monthly Weather Review*, *149*(7), 2097–2113. https://doi.org/10.1175/MWR-D-20-0333.1